International Microbiology
https://doi.org/10.1007/s10123-024-00628-1

RESEARCH

The effects of nickel tungstate nanoparticles ($NiWO_4$ NPs) on freshwater microalga *Raphidocelis subcapitata* (Chlorophyceae)

Cínthia Bruno de Abreu[1] · Renan Castelhano Gebara[1] · Giseli Swerts Rocha[2] · Adrislaine da Silva Mansano[3] · Marcelo Assis[4] · Thalles Maranesi Pereira[5] · Luciano Sindra Virtuoso[5] · Ailton José Moreira[6] · Mykaelli Andrade Santos[7] · Maria da Graça Gama Melão[3] · Elson Longo[1]

Received: 5 June 2024 / Revised: 17 November 2024 / Accepted: 19 December 2024

Abstract
Among the vast array of functional nanoparticles (NPs) under development, nickel tungstate ($NiWO_4$) has gained prominence due to its potential applications as a catalyst, sensor, and in the development of supercapacitors. Consequently, new studies on the environmental impact of this material must be conducted to establish a regulatory framework for its management. This work aims to assess the effects of $NiWO_4$ (NPs) on multiple endpoints (e.g., growth, photosynthetic activity, and morphological and biochemical levels) of the freshwater microalga *Raphidocelis subcapitata* (Chlorophyceae). Quantification data revealed that the fraction of dissolved Ni and free Ni^{2+} increased proportionally with $NiWO_4$ NP concentrations, although these levels remained relatively low. Biological results indicated that $NiWO_4$ NPs did not inhibit the growth of algal cells, except at 7.9 mg L^{-1}, resulting in a 9% decrease. Morphological changes were observed in cell size and complexity, accompanied by physiological alterations, such as a reduction in chlorophyll *a* fluorescence (FL3-H) and signs of impaired photosynthetic activity, indicated by the effective quantum yield, quenchings, and chlorophyll *a* (Chl *a*) content. Furthermore, the rapid light curves showed that the NPs in high concentrations affected microalga ability to tolerate high light intensities, as corroborated by the significant decrease in the relative electron transport rate (rETRmax) and saturation irradiance (Ek). Based on the present study results, we emphasize the importance of applying integrative approaches in ecotoxicological studies, since each endpoint evaluated showed different sensitivity.

Keywords Nickel tungstate · Nanoparticles · Ecotoxicology · *Raphidocelis subcapitata* · Freshwater ecosystem

Introduction

Nanoparticles (NPs) based on tungstates have gained significant attention due to their multifunctional applications as catalysts, photocatalysts, batteries, and lasers and in the development of biomaterials (Ke et al. 2018; Assis et al. 2023). Their versatility lies in internal charge transitions, as well as their ability to associate with other metals, forming structures such as MWO_4 and M_2WO_4 (M = metal) (Montini et al. 2010; Ungelenk et al. 2014). In particular, nickel

✉ Cínthia Bruno de Abreu
cinthiaabreu123@gmail.com

[1] Center for the Development of Functional Materials (CDMF), Universidade Federal de São Carlos (UFSCar), Rodovia Washington Luís, Km 235, São Carlos, SP 13565-905, Brazil

[2] Departament Enginyeria Química, Escola Tècnica Superior d'Enginyeria Química, Universitat Rovira I Virgili, Av. Països Catalans, 26. 43007, Tarragona, Spain

[3] Department of Hydrobiology, Universidade Federal de São Carlos (UFSCar), Rodovia Washington Luís, Km 235, São Carlos, SP 13565-905, Brazil

[4] Biomaterials and Bioengineering Lab, Translational Research Centre San Alberto Magno, Catholic University of Valencia San Vicente Mártir (UCV), 46001 Valencia, Spain

[5] Chemistry Institute, Universidade Federal de Alfenas (UNIFAL-MG), Gabriel Monteiro da Silva, Alfenas, MG 70037130-000, Brazil

[6] Chemistry Institute, Universidade Estadual Paulista (UNESP), Araraquara, SP, Brazil

[7] Department of Chemistry, Universidade Federal de São Carlos (UFSCar), Rodovia Washington Luís, Km 235, São Carlos, SP 13565-905, Brazil

Published online: 09 January 2025

tungstate ($NiWO_4$) has been prominent, especially in its nanoparticle form, due to its optical, electrical, and magnetic properties (López et al. 2016; Shanmugapriya et al. 2016). It is employed in the development of new catalysts, photocatalysts, photovoltaic and electrochemical cells, pigment additives, and humidity and gas sensors and as an antimicrobial material (Montini et al. 2010; Pourmortazavi et al. 2012; Azadbakht et al. 2013; Mohamed et al. 2014; Karthiga et al. 2015; López et al. 2016; Mani et al. 2016; AlShehri et al. 2017; Li et al. 2017). The increasing integration of technologies employing $NiWO_4$ NPs, combined with a commitment to environmental responsibility, highlights the need for in-depth studies on the ecotoxicological effects of this material, especially in aquatic ecosystems. Such research is crucial for establishing comprehensive regulatory frameworks governing its utilization, disposal, and recycling.

One aspect to consider in the toxicity of inorganic NPs, such as $NiWO_4$, is the dissolution of their ions (Nguyen et al. 2020). Various nanotoxicity studies suggest that the adverse effects of metallic NPs on aquatic organisms are primarily caused by the release of ions, rather than solely by the inherent characteristics of the NPs (Bundschuh et al. 2016; Levard et al. 2012; Zhang et al. 2019). Therefore, understanding the quantity of ions released from the nanoparticles into the solution is essential to support the results of toxicity tests. In the case of the metallic nanoparticles, this release process may be more pronounced due to their larger surface area (Levard et al. 2012; Zhang et al. 2019).

The potential toxicity of $NiWO_4$ NPs to aquatic biota, particularly freshwater microalgae, remains unknown. Since these NPs can be directly introduced into an aquatic environment, absorbed by soil, and transported to aquatic ecosystems via surface runoff or wastewater (Oukarroum et al. 2015), biota may be exposed to both $NiWO_4$ NPs and the Ni^{2+} ions they release. Concerns have been raised regarding the release of Ni^{2+} through Ni-based NPs. Although this metal is naturally present in the environment, NPs could serve as an additional source of Ni, which could have adverse effects on aquatic organisms. Specifically, for microalgae, Ni has been linked with changes in cell density, the generation of reactive oxygen species (ROS), and alterations in metabolic processes (Martínez-Ruiz and Martínez-Jerónimo 2015; Reis et al. 2024). In general, the negative effects of Ni-based NPs on various microalgae species encompass alterations in population levels, such as growth inhibition, disruptions in physiological processes (e.g., changes in the photosynthetic apparatus), and the induction of oxidative stress (Gong et al. 2014; Oukarroum et al. 2017; Sousa et al. 2018).

Given the role of microalgae in aquatic ecosystems, where they contribute to carbon fixation and oxygen production, this study focused on using the unicellular species *Raphidocelis subcapitata* (Chlorophyceae) as a model organism. This species is known for its rapid growth, ecological relevance, sensitivity to various contaminants, and widespread use in ecotoxicological tests involving NPs (Nogueira et al. 2015; Alho et al. 2020; Abreu et al. 2022a, 2022b). *R. subcapitata* is widely found in aquatic environments around the world and is recommended by regulatory agencies as a model organism. Additionally, it has diverse applications in biotechnology, including the production of biofuels such as biogas, third-generation biodiesel, and bioethanol. The species is also used in wastewater bioremediation to remove pollutants, nutrients, and inorganic compounds, as well as in the development of products for human food and animal nutrition (Machado and Soares 2024).

Based on this, our aim was to adopt an integrated approach using multiple endpoints, including morphological, physiological, and biochemical parameters assessed through flow cytometry, pulse amplitude modulated (PAM) fluorometry, and determination of chlorophyll *a* (Chl *a*) content, in order to evaluate the effects of $NiWO_4$ on microalgae *R. subcapitata.* Also, we investigated the Ni dissolved and ionic release of Ni^{2+} as well as the aggregation of NPs across all treatments. This is the first study to explore the effects of $NiWO_4$ nanoparticles on a photosynthetic organism. Understanding these effects is essential for ensuring the responsible and cautious use of tungstate-based nanoparticles. Furthermore, our findings provide valuable insights that can help shape the development of standards and regulations for safe nanoparticle concentrations in freshwater ecosystems, supporting their protection and conservation.

Materials and methods

Synthesis and characterization

$NiWO_4$ NPs were synthesized using the coprecipitation method followed by microwave-assisted hydrothermal irradiation. Details of the synthesis, characterization, metal determination, and ionic release can be found in the Supplementary Material.

R. subcapitata culture and toxicity tests

R. subcapitata was obtained from stock cultures at Ecotoxicology Laboratory at the Federal University of São Carlos, SP, Brazil (Mansano et al. 2017) and cultured in an L.C. Oligo culture medium (AFNOR, 1980) (Table S1, Supplementary material) at 25 ± 1 °C, with ≅ 130 µmol photon m^{-2} s^{-1} LED light and 12 h/12 h of light/dark photoperiod. The initial pH was around 7. The NP stock solutions were prepared immediately before the experiments and dispersed in ultrapure water using a bath sonicator (Ultra cleaner 1400 Unique) for 30 min. The test solutions were then prepared

by adding the NPs to the algal culture medium. Algal cultures in the exponential growth phase were inoculated at a concentration of 1×10^5 cells mL^{-1} in 500 mL polycarbonate Erlenmeyer flasks containing 250 mL of test solutions. *R. subcapitata* was exposed for 96 h to concentrations of 0.00 (control), 7.9, 15.8, 39.6, 55.4, and 79.1 mg L^{-1}, with triplicates for each concentration.

To determine the cell density, we sampled 1.8 mL aliquots daily, which were fixed with formaldehyde (1% final concentration). Samples were left in the dark for 10 min, frozen in nitrogen liquid, and were kept at − 20 °C until analysis. To determine intracellular ROS, we used 495 µL of each sample and 5 µL of DCFH-DA (2′7′-dichlorofluorescein diacetate, Sigma Aldrich) with a final concentration of 10 µM. Then, the samples were kept in the dark for 60 min and immediately analyzed by flow cytometry. A FACSCalibur cytometer (Becton Dickinson, San Jose, CA, USA) with a 15 mW argon-ion laser (488 nm excitation) was used for this analysis, and 6-µm fluorescent beads (Fluoresbrite carboxylate microspheres; Polysciences, Warrington, Pennsylvania, USA) served as an internal standard.

The algal cells were identified according to Sarmento et al. (2008) using the side scatter (SSC–H) versus red fluorescence (FL3-H) parameters. For ROS analysis, the parameters FL3-H and FL1-H (green fluorescence) were used. Additionally, SSC-H (cell complexity), the relative values of FL3-H (Chl *a* fluorescence), and FSC-H (cell size) of microalga were calculated according to Mansano et al. (2017). The data were analyzed using FlowJo V10 software (Treestar.com, USA), and the equations established by Hong et al. (2009) were applied to calculate relative ROS levels.

To evaluate the photosynthetic activity, we used a PAM fluorometer (Phyto-PAM® Fluorometer Analyzer, Heinz Walz, Germany). Every day, we sampled 3 mL of each replicate, which was kept in the dark for 15 min to promote oxidation of the photosystem II (PSII) reaction centers. Afterward, the photosynthetic parameters of dark-adapted algal cells were evaluated (Herlory et al. 2013). The Phyto-PAM provided the values for minimum fluorescence (F_0), maximum fluorescence (F_M), and maximum quantum yield (ΦM) (Schreiber, 1986; Schreiber et al. 1995). From these values, the equation F_0/F_V (where $F_V = F_M - F_0$) (Kriedemann et al. 1985) was used to calculate the efficiency of the oxygen evolving complex (OEC).

At 72 h, to obtain the parameters of light-adapted cells, the samples were exposed to continuous actinic light. The equipment then provided data on variable fluorescence (F_S) and the maximum fluorescence of light-adapted cells (F_M'). Using these parameters, we calculated the effective efficiency of PSII = $(F_M' - F_S) / F_M'$ (Genty et al. 1989; Baker 2008; Cosgrove and Borowitzka 2010). We also used these parameters to calculate the photochemical (qP) and non-photochemical (qN, NPQ, Y(NPQ) and Y(NO)) quenching, according to the equations provided in Table S2 (Supplementary material).

At 72 h, we also obtained rapid light saturation curves using the PAM fluorometer, by increasing the intensity of photosynthetically active radiation (PAR) up to 1780 µmol photons m^{-2} s^{-1} with a 20-s light pulse, according to Rocha et al. (2021). From these data, we calculated the relative electron transport rate (rETR; µmol electrons m^{-2} s^{-1}), and with the rETR and PAR data, we fitted the light saturation curve using the Jassby and Platt (1976) equation. The initial slope (α) and the maximum relative rate of electron transport (rETRmax; µmol electrons m^2 s^{-1}) were obtained, and the saturating irradiance (*Ek*) was calculated as $Ek = \text{rETRmax}/\alpha$; µmol photons m^{-2} s^{-1} (Rocha et al. 2021).

Finally, after 96 h of exposure, to determine chlorophyll *a* content, we used the methodology described by Shoaf and Lium (1976) to extract the pigment and the equation described by Jeffrey and Humphrey (1975) to quantify chlorophyll *a* content.

Data treatment and statistical analysis

To assess the differences between the control and treatments groups, normally distributed data were analyzed using one-way ANOVA, followed by Dunnett's post hoc multiple-comparison test. For non-normal distributed data, the Kruskal–Wallis test and multiple comparisons with Dunn's test were performed. The level of statistical significance was defined as $p < 0.05$.

Results and discussion

Characterization of $NiWO_4$ NPs and ion release

To assess the success of $NiWO_4$ nanoparticle synthesis and characterize the size of the synthesized NPs, X-ray diffraction (XRD), Raman spectroscopy, and transmission electron microscopy (TEM) analyses were conducted (Fig. 1). The XRD patterns reveal that $NiWO_4$ has a monoclinic structure, belonging to the P2/c spatial group, in accordance with the crystallographic card number 1879016 from the Inorganic Crystal Structure Database (ICSD) (Rosal et al. 2018). No additional peaks related to secondary phases were observed, indicating the high purity of the synthesized NPs. Additionally, the sample exhibits high crystallinity, as evidenced by the sharp and intense peaks. As a complementary analysis to XRD, Raman spectroscopy highlights the monoclinic wolframite-type structure of $NiWO_4$, displaying Raman modes associated with this structure (Ibiapina et al., 2022). Examining the FE-SEM images of the sample reveals that

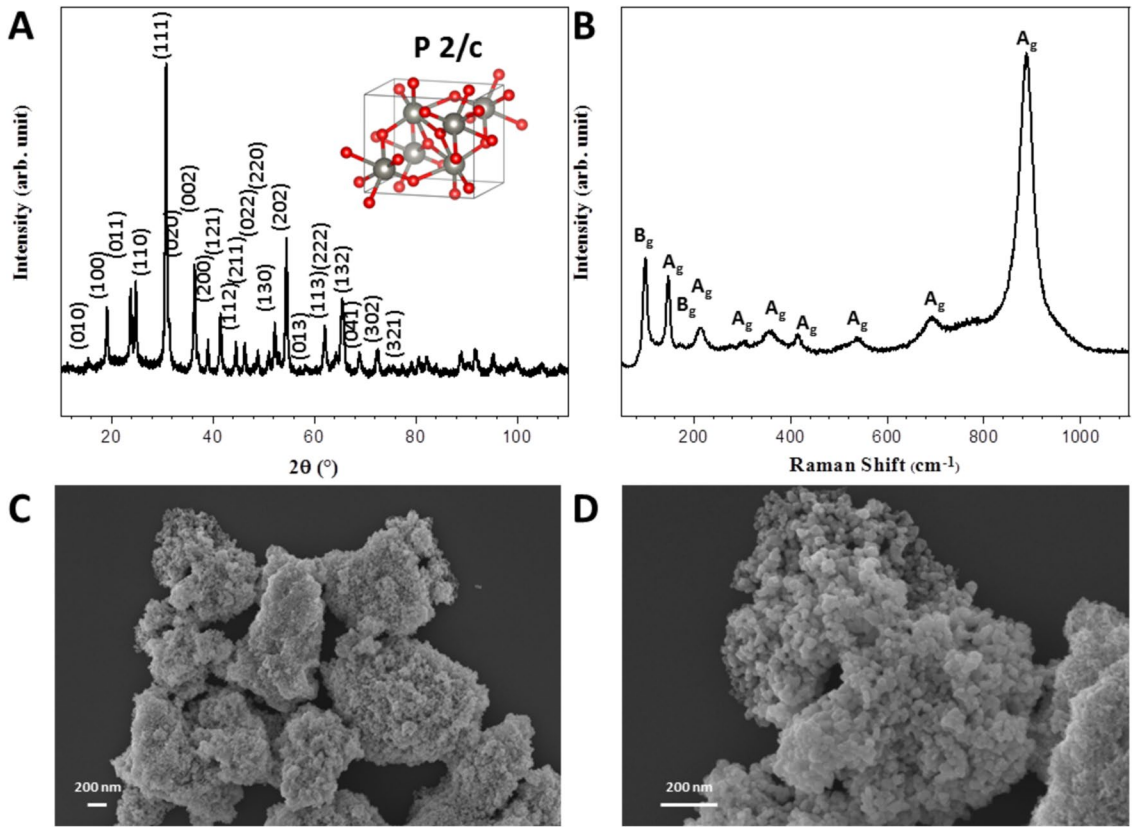

Fig. 1 **(a)** XRD, (**b**) Raman spectrum, and (**c**, **d**) FE-SEM images of $NiWO_4$ nanoparticles

the morphology of $NiWO_4$ NPs consists of irregular polyhedra with an average size of 19.7 ± 4.6 nm.

After analyzing the solid-phase behavior of the material, the analyses of $NiWO_4$ NPs in the solution were conducted using ultrapure water and the culture medium employed for the growth of microalgae. The hydrodynamic sizes of NPs in the culture medium, as shown in Table 1, are larger than the average diameters of individual particles obtained by FE-SEM and differ from the hydrodynamic size of NPs in water, which can be attributed to the aggregation of NPs. In the culture medium, the NPs exhibit sizes of 501.33 ± 120.85, 580 ± 88.94, and 463.77 ± 93.98 nm at concentrations of 39.6, 55.4, and 79.1 mg L^{-1}, respectively, indicating a greater degree of aggregation in the culture medium compared to the ultrapure water. Several factors in the aqueous medium influence the aggregation of NPs, including pH, concentration, ionic strength, and composition of the medium (Oukarroum et al., 2012). The polydispersity index (PdI) varied from 0.19 ± 0.01 at the lowest concentration (7.9 mg L^{-1}) to 0.34 ± 0.12 at 55.4 mg L^{-1} (Table 1). This index reflects the particle size distribution in the solution and can range from 0.01, indicating monodispersity, to 0.5–0.7 (Danaei et al. 2018). According to Lemarchand et al. (2003), PdI values below or around 0.3 suggest that particles dispersed in the solution exhibit a homogeneous size distribution. Therefore, based on our data, we can infer that $NiWO_4$ NPs are homogeneous at all tested concentrations.

The zeta potential results in ultrapure water and culture medium are presented in Table 1. According to Stensberg et al. (2011), suspensions are considered stable in aqueous solutions if their zeta potential values are above +30 mV and below −30 mV. Based on the zeta potential at concentrations of 7.9 and 15.8 mg L^{-1}, the $NiWO_4$ NPs exhibit moderate stability. In contrast, at concentrations of 39.6, 55.4, and 79.1 mg L^{-1}, the NPs are unstable.

The release of Ni^{2+} ions occurred proportionally to the increase in $NiWO_4$ NP concentrations (Table 1). It is known that the release of ions from NPs in aqueous media depends on factors such as the methodology used in the synthesis and the size, shape, and surface area of the NPs (Lekamge et al. 2020). Authors, such as Beer et al. (2012), Dobias and Bernier-Latmani (2013), and Sendra et al. (2017), have pointed out that NPs have a high dissolution capacity due to their large surface area. In this study, we observed the presence of dissolved Ni and free Ni in the treatments; however, when compared to the $NiWO_4$ concentrations, the release of Ni^{2+} is minimal. This effect is related to the greater

Table 1 Characterization parameters of $NiWO_4$ NPs in ultrapure water and LC Oligo medium; dissolved nickel (in all treatments) and free nickel ions released (at the lowest, intermediate and highest concentrations) from different concentrations of $NiWO_4$ NPs in LC Oligo medium

$NiWO_4$ (mg L^{-1})	Hydrodynamic size (nm)		PdI		Zeta-potential (mV)	Hydrodynamic size (nm)	PdI	Zeta-potential (mV)	Nickel (mg L^{-1})	Ni^{2+} (mg L^{-1})
	Ultrapure water					L.C Oligo			Dissolved	Free ion
7.9	147.4 ± 8.5	0.19 ± 0			−38.27 ± 0.7	155.2 ± 2.8	0.19 ± 0	40.3 ± 1.4	0.034 ± 0	0.004 ± 0
15.8	161.43 ± 2.6	0.31 ± 0			−34 ± 1	159.6 ± 5	0.19 ± 0	33.53 ± 0.3	0.063 ± 0	
39.6	163.8 ± 1.3	0.31 ± 0			−36.9 ± 0.6	501.3 ± 120.8	0.25 ± 0	4.83 ± 7.6	0.131 ± 0	0.020 ± 0
55.4	153.07 ± 5.4	0.27 ± 0			−35.67 ± 0.35	580 ± 88.9	0.34 ± 0	−17.5 ± 4.5	0.161 ± 0	
79.1	160.33 ± 2.3	0.31 ± 0			−37.8 ± 0.2	463.8 ± 93.9	0.33 ± 0	−19.53 ± 0.4	0.210 ± 0	0.034 ± 0

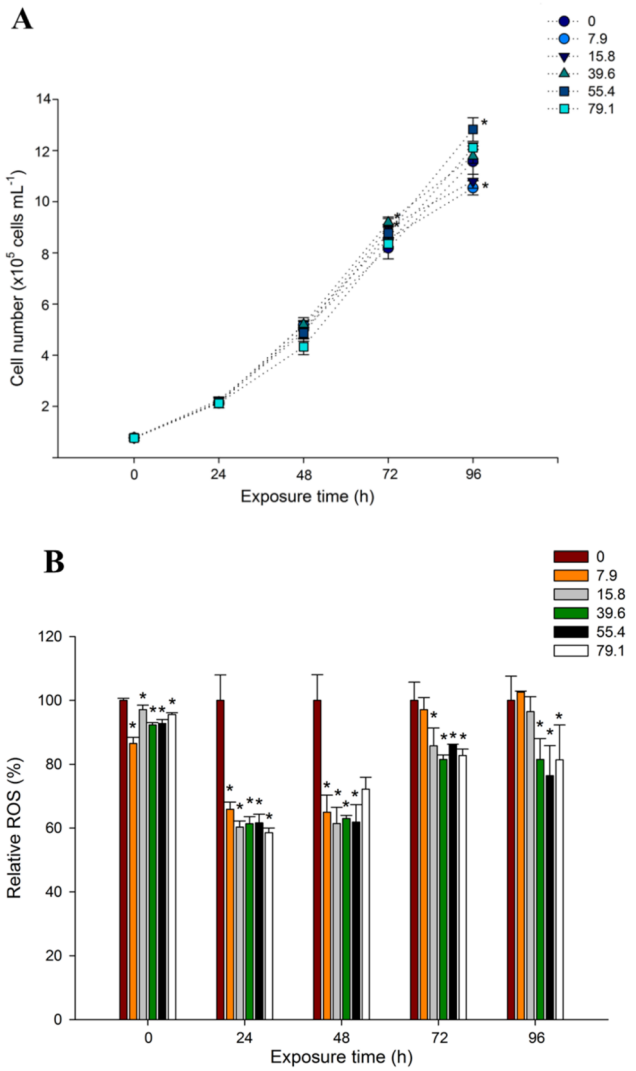

Fig. 2 Average growth (**a**) and reactive oxygen species (ROS) (**b**) produced by *R. subcapitata* exposed to $NiWO_4$ NPs. Error bars represent the standard deviation, and asterisks represent a significant difference ($p < 0.05$) of treatments compared to the control group. Concentrations are expressed in mg L^{-1}. Separate statistical analyses were performed for each day of exposure

stability of $NiWO_4$ in the solution compared to other Ni-based materials.

Ecotoxicity results

In general, the $NiWO_4$ NPs did not negatively affect algal cell growth (Fig. 2a), and thus, it was not possible to calculate the IC_{50}. At 72 h, concentrations of 15.8 mg L^{-1} and 39.6 mg L^{-1} resulted in a slight increase in cell density when compared to the control. Only at 96 h, when compared to the control, did we observe a reduction of approximately 9% in cell density at the lowest concentration (7.9 mg L^{-1}). Additionally, at a concentration of 55.4 mg L^{-1}, we observed

an increase of approximately 12% in cell density when compared to the control.

Cell growth rates are closely linked to survival and are therefore considered a universal endpoint (Barreto et al. 2021). Our cell growth data differ from some toxicity studies based on this endpoint and with other Ni-based NPs. For example, the same species used as a test organism in this study had its growth compromised when exposed to NiO NPs with a size between 5 and 20 nm, showing an $LC_{50–96\,h}$ of 0.35 mg L^{-1} (Griffitt et al. 2008). Also, Nogueira et al. (2015) obtained an $EC_{50–72\,h}$ of 15.2 mg L^{-1} for NiO NPS with a size between 10 and 20 nm and an $EC_{50–72\,h}$ of 8.24 mg L^{-1} for larger particles and also concluded that the toxicity was caused by the availability of Ni^{2+} ions. In contrast, Sousa et al. (2018) showed a lower $EC_{50–72\,h}$ (1.6 mg L^{-1}) for NiO whose size was less than 50 nm. Gong et al. (2011) determined a $EC_{50–72\,h}$ of 32.28 mg L^{-1} and verified the growth inhibition of *Chlorella vulgaris* exposed to NiO. This value is relatively close to the $EC_{50–96\,h}$ of 40.8 mg L^{-1} determined by Han and Zhang (2012) for the same species. These findings suggest that the negative effects of Ni NPs on different organisms and the concentrations that inhibit cell growth vary depending on the species tested, the characteristics of NPs (e.g., size), and its relationship with the release of Ni^{2+} ions.

In the literature, it has been described that the main damages caused by NPs to organisms affect the cell membranes and nucleic acids (DNA and RNA), in addition to causing cellular damage due to excess ROS and oxidative stress (Gong et al. 2014; Azqueta and Dusinska, 2015; Marisa et al., 2015), which compromises physiological and metabolic functions. Therefore, we evaluated the amount of intracellular ROS produced by algal cells exposed to $NiWO_4$ NPs (Fig. 2b) and observed that in the first hour of exposure (1 h) to the NPs, there was a significant reduction of approximately 15% of ROS at 7.9 mg L^{-1} and around 10% in other treatments. At 24 h and 48 h, the decrease in ROS was ~ 40% in treatments, when compared to the control. At the end of exposure, algal cells exposed to the $NiWO_4$ produced significantly less ROS than the control. These results suggest the significantly lower intracellular ROS levels in *R. subcapitata* cells exposed to different concentrations of $NiWO_4$ NPs which corroborates our findings of no growth inhibition at most $NiWO_4$ NPs concentrations. It is also interesting to note that this reduction in the intracellular ROS is also corroborated by our cell size data (discussed below). We highlight the possible activation of antioxidant enzymes in algal cells (Martínez-Ruiz and Martínez-Jerónimo 2015; Lekamge et al., 2019; Gebara et al. 2020). While we did not quantify the antioxidant enzymes, it is well established that microalgae activate this antioxidant system in response to stress caused by different contaminants (Lekamge et al., 2019; Qian et al. 2016), particularly when exposed to metallic NPs.

Another important aspect to consider is the release of ions from the NPs, which can interact with biological systems (Levard et al 2012; Oukarroum et al. 2015; Nogueira et al. 2015). As previously mentioned, the small size of the particles and the release of ions are widely discussed in toxicity studies (Bian et al. 2011; Levard et al. 2012; Zhang et al. 2019). As shown in Table 1, the concentration of dissolved Ni in the treatments ranged from 0.0034 ± 0.00026 to 0.210 ± 0.002712 mg L^{-1}, and the concentration of free Ni^{2+} ranged from 0.004 to 0.034 mg L^{-1}, representing only 0.04% of Ni^{2+} at highest concentration.

In addition, aggregation of the $NiWO_4$ NPs was observed, which can directly interfere with the dissolution of NPs. Even when high concentrations of NPs were used in the ecotoxicity tests, the availability of dissolved Ni in the solution was relatively lower than of Ni^{2+} concentrations that cause negative damage to *R. subcapitata*. Reis et al. (2024) observed an increase in growth at 0.10 mg L^{-1} of Ni, a result similar to that found in this study, since at 55.4 mg L^{-1} of $NiWO_4$, the amount of dissolved Ni was 0.161 mg L^{-1}. The concentrations of Ni that cause effects on different species of microalgae vary, depending on the species. For instance, Filová et al. (2021) established an IC_{50} of 0.50 Ni mg L^{-1} for *R. subcapitata*, which is much higher than the concentrations of dissolved Ni and free Ni^{2+} available in the $NiWO_4$ treatments evaluated in this study. For other microalgae species when exposed to Ni, according to Martínez-Ruiz and Martínez-Jerónimo (2015), the $IC_{50–96\,h}$ for *Ankistrodesmus falcatus* was 0.017 mg L^{-1}; Peters et al. (2018) determined an EC_{50} of 2.41 mg Ni L^{-1} for *Chlorella* sp.; an $EC_{50–96\,h}$ of 1.85 ± 0.17 mg Ni L^{-1} was determined for *Phaeodactylum tricornutum* (Guo et al. 2022); and Panneerselvam et al. (2018) determined an $IC_{50–96\,h}$ of 0.31 ± 0.01 mg L^{-1} Ni for *Odontella mobiliensis*.

Regarding morphological endpoints, we observed changes in cell complexity (SSC-H) and cell size (FSC-H) compared to the control (Fig. 3a, b). The algal cells exposed to $NiWO_4$ NPs exhibited varying responses throughout the exposure period. In the initial hours, SSC-H increased significantly (Dunnett's test, $p < 0.05$) only at 55.4 mg L^{-1}. At 72 h, SSC-H significantly decreased (Dunnett's test, $p < 0.05$) from 15.8 mg L^{-1}. At the end of exposure (96 h), SSC-H had increased significantly at concentrations of 7.9 and 15.8 mg L^{-1}, but decreased significantly at the highest concentrations (55.4 and 79.1 mg L^{-1}). The increase in SSC-H observed at the lowest concentrations (7.9 and 15.8 mg L^{-1}) is probably a result of the internalization of Ni^{2+}. Previous, studies have also observed an increased in cell complexity and ion internalization by algal cells (Suzuki et al. 2007; Gebara et al. 2020; Abreu et al. 2022a). These changes may reflect a detoxification mechanism through the internalization of toxic components within the cells (Almeida et al., 2019). Therefore, our results showing an

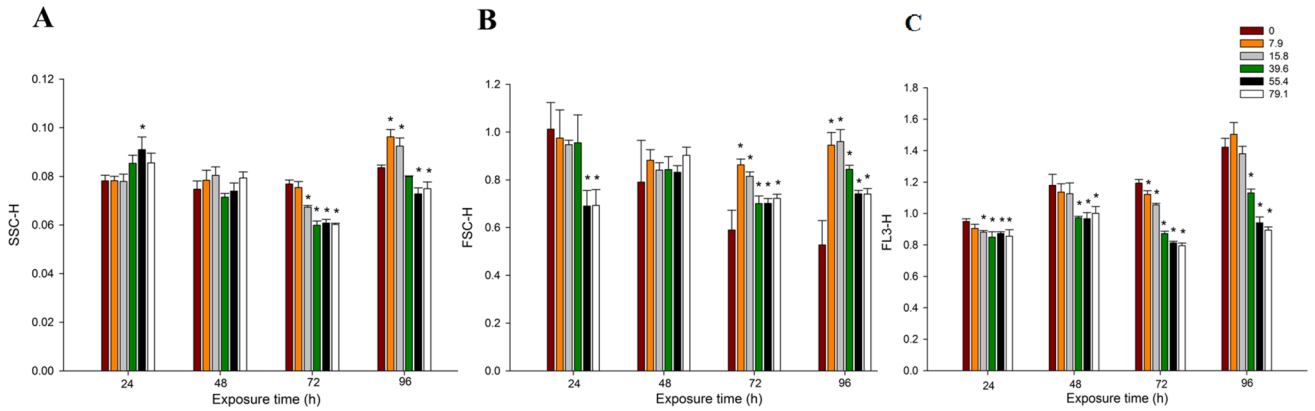

Fig. 3 Cellular complexity (SSC-H) (**a**), cell size (FSC-H) (**b**), and chlorophyll *a* fluorescence (FL3-H) (**c**) of *Raphidocelis subcapitata* exposed to $NiWO_4$ NPs. Concentrations are expressed in mg L^{-1}, and the asterisks represent a significant difference ($p < 0.05$) of treatments compared to the control group. Separate statistical analyses were performed for each day of exposure

increase in SSC-H at the lowest concentration (7.9 mg L^{-1}) corroborate our cell density data, which indicated that the growth of *R. subcapitata* was inhibited by approximately 9%. On the other hand, the opposite occurred with the 55.4 mg L^{-1} treatment, since cell complexity decreased and cell growth increased by 12%.

The size of the algal cells, as indicated by FSC-H (Fig. 3b), decreased significantly (Dunnett's test, $p < 0.05$) only at the highest concentrations (55.4 and 79.1 mg L^{-1}) after 24 h of exposure to the $NiWO_4$. In contrast, at 72 h and 96 h, cell size increased significantly (Dunnett's test, $p < 0.05$) in all treatments compared with the control. Several studies have reported an increase in the cell size of *R. subcapitata* exposed to various types of contaminants (Gebara et al. 2020; Machado and Soares 2014; Mansano et al. 2017; Souza et al. 2018; Reis et al. 2022). Bryan et al. (2012) suggests that cell size is directly related to the cell cycle and is influenced by different stimuli. Machado and Soares (2014) highlight that cell size is a crucial aspect for unicellular algae to maintain proper cell division.

Regarding Chl *a* fluorescence (FL3-H), we observed a statistically significant decrease (Dunnett's test, $p < 0.05$) (Fig. 3c). Specifically, after 24 h, Chl *a* fluorescence decreased from 15.8 mg L^{-1}, after 48 h, from 39.6 mg L^{-1}, at 72 h, at all the concentrations tested; and finally, at 96 h, from 39.6 mg L^{-1}. It is known that fluorescence measured with the FL3-H detector can be used to assess the physiology of algal cells and that a reduction in FL3-H indicates potential problems in the synthesis of pigments in cells exposed to contaminants (Sendra et al. 2017). The reduction in FL3-H of *R. subcapitata* cells exposed to $NiWO_4$ was a sensitive endpoint, especially after 48 h, suggesting impaired photosynthetic performance in the microalgae. Interestingly, at 72 h and 96 h, although FL3-H was reduced, our Phyto-PAM data indicated that the photosynthetic activity was only subtly compromised at 39.6 mg L^{-1} and 79.1 mg L^{-1}.

With regard to the photosynthetic activity parameters obtained with Phyto-PAM, a slight decrease in maximum quantum yield (Fig. 4a) was observed only after 48 h of exposure, at concentrations of 15.8 mg L^{-1} (1.42% decrease), 39.6 mg L^{-1} (2% decrease), and 55.4 mg L^{-1} (2.38% decrease), which are corroborated by the reduction in FL3-H. It should be noted that although a statistical difference was observed, this decrease in maximum yield (around 2%) may not represent a physiological significant change. At 72 h and 96 h, we observed that the maximum yield was not compromised, which may indicate that the algal cells had recovered from the physiological stress induced by the $NiWO_4$ NPs. The maximum quantum yield reflects the physiological health of microalgae (Herlory et al. 2013), by measuring the amount of light used in photosynthesis. According to our data, the algal cells exposed to $NiWO_4$ showed no changes in PSII's ability to carry out primary photochemical reactions (Dewez and Oukarroum, 2012).

On the other hand, when we examined the F_0/F_v parameter (Fig. 4b), we observed a significant increase of around 5.5% at the 79.1 mg L^{-1} during the first few hours of exposure. At 48 h, F_0/F_v increased at 15.8, 39.6, 55.4, and 79.1 mg L^{-1}. No significant changes were observed at 72 h and 96 h at any of the concentrations tested. This parameter indicates the efficiency of the oxygen evolving complex (OEC) and according to Matto et al. (1999), the OEC is part of the water splitting system, where the water molecule is broken down in the presence of light, resulting in the production of oxygen (Mattoo et al. 1999). Increased F_0/F_v values may indicate damages to the water splitting apparatus, as shown by Alho et al. (2019), Reis et al. (2021), Abreu et al. (2022b), and Gebara et al. (2023). Therefore, we can infer that the water splitting apparatus was not a major target

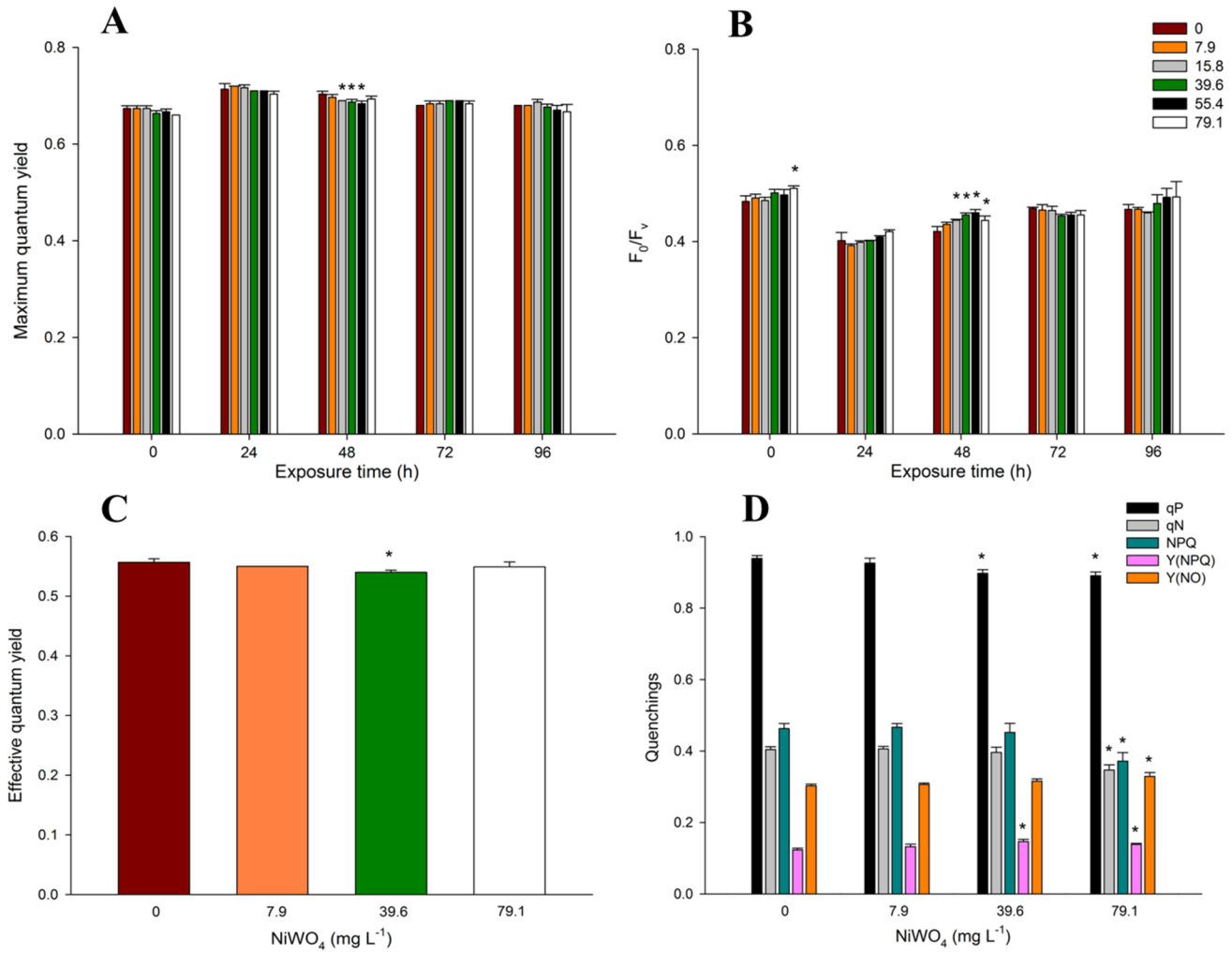

Fig. 4 Maximum quantum yield (**a**), measurement of the efficiency of oxygen evolving complex (F_0/F_V) (**b**), effective quantum yield (**c**), and quenchings (**d**) of *R. subcapitata* exposed to $NiWO_4$ NPs. Concentrations are expressed in mg L^{-1}, and the asterisks represent a significant difference ($p < 0.05$) of treatments compared to the control group. Separate statistical analyses were performed for each day of exposure

of the $NiWO_4$ NPs, since the F_0/F_v values did not increase significantly during most of the exposure period. The small changes observed at 48 h and the lack of significant changes in both maximum yield and F_0/F_v endpoints during the later hours of exposure further suggest possible recovery of algal cells after the stress caused by the $NiWO_4$. These results also corroborate the absence of growth inhibition, as photosynthetic activity, measured via Phyto-PAM, was generally not compromised. We highlight that these endpoints in evaluating the toxicity of $NiWO_4$ NPs to *R. subcapitata* may not be sensitive enough to detect any damage to algal cells. Unlike this, morphological changes in cell complexity and size, as well as chlorophyll *a* fluorescence, were more sensitive endpoints, as they exhibited changes measurable. However, when we consider the photosynthetic parameters, obtained via Phyto-PAM measured at 72 h, we observed significant reductions ($p < 0.05$) in the effective quantum yield at 39.6 mg L^{-1} (Fig. 4c).

The photochemical quenching (qP) (Fig. 4d) decreased by 4.44% and ~ 5.13% (Dunnett's test, $p < 0.05$) at 39.6 and 79.1 mg L^{-1} of $NiWO_4$, respectively, indicating that reaction centers may have closed, compromising carbon assimilation (Rocha et al. 2021). This is because, according to Rocha et al. (2021), qP reflects the proportion of PSII reaction centers that are open. Non-photochemical quenching (qN, NPQ, *Y*(NPQ), *Y*(NO)) data are shown in Fig. 4d. At 79.1 mg L^{-1} qN decreased (Dunnett's test, $p < 0.05$) by 14.2% and NPQ decreased (Dunnett's test, $p < 0.05$) by 19.64%. On the other hand, we observed significant increases (Dunnett's test, $p < 0.05$) in Y(NPQ) of around 18.8% at 39.6 mg L^{-1} and 12.16% at 79.1 mg L^{-1}, while Y(NO) increased by ~ 8.8% at 79.1 mg L^{-1}. These results suggest that algal cells exposed

to the highest concentration of $NiWO_4$ NPs had an increase in the dissipation of unregulated energy, in the form of heat and fluorescence, as corroborated by the increase in Y(NO) (Klughammer and Schreiber 2008). Additionally, damage to the photoprotection mechanism may have occurred, since NPQ was reduced at the highest $NiWO_4$ concentration (79.1 mg L^{-1}). The increase in Y(NPQ) indicates activation of photoprotection mechanisms (active), but there appears to be a decrease between 39.6 and 79.1 mg L^{-1}, accompanied by a reduction in NPQ and qN, as well as an increase in Y(NO). This may indicate the onset of damage to photoprotection mechanisms.

The rapid light curve parameters of *R. subcapitata* exposed to $NiWO_4$ NPs are shown in Fig. 5. The NPs significantly decreased (Dunnett's test, $p < 0.05$) the $rETR_{max}$ at 39.6 and 79.1 mg L^{-1}, indicating an inhibition of the electron transport rate (Fig. 5a). The $NiWO_4$ did not affect alpha (Fig. 5b) but reduced (Dunn's test, $p < 0.05$) the saturation irradiance only at 79.1 mg L^{-1}, as shown by E_k (Fig. 5c). These results highlight that at these concentrations, the NPs impaired the algal cells' ability to tolerate high light intensities.

Regarding biochemical endpoint (Fig. 6), we observed a trend towards a reduction in Chl *a* content. However, the reductions were only significant (Dunnett's test, $p < 0.05$)

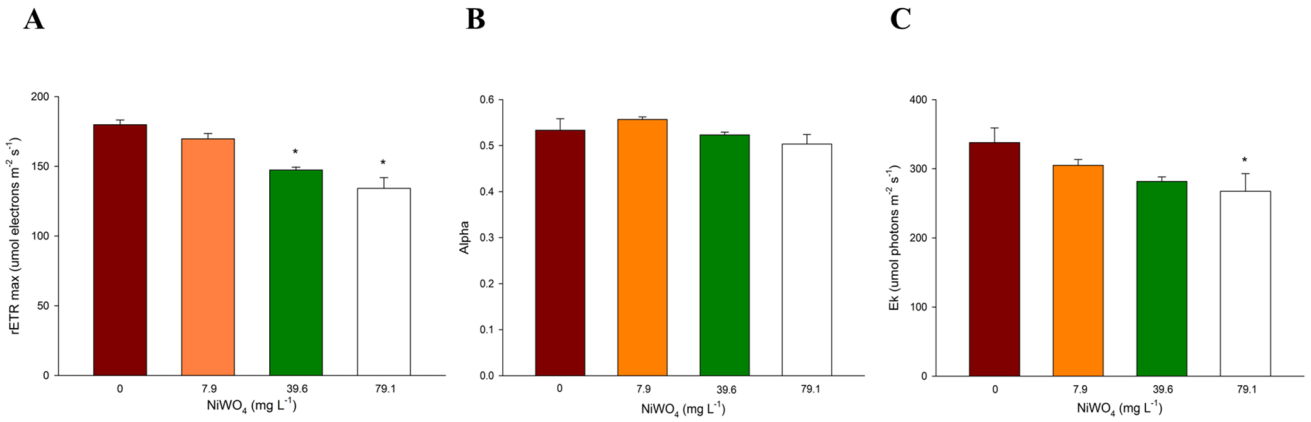

Fig. 5 Light curve parameters of *R. subcapitata* exposed to $NiWO_4$ nanoparticles. Electron transport rate – rETRmax (µmol electrons m^{-2} s^{-1}) (**a**), alpha (**b**), and saturation irradiance – *Ek* (µmol electrons m^{-2} $s.^{-1}$) (**c**)

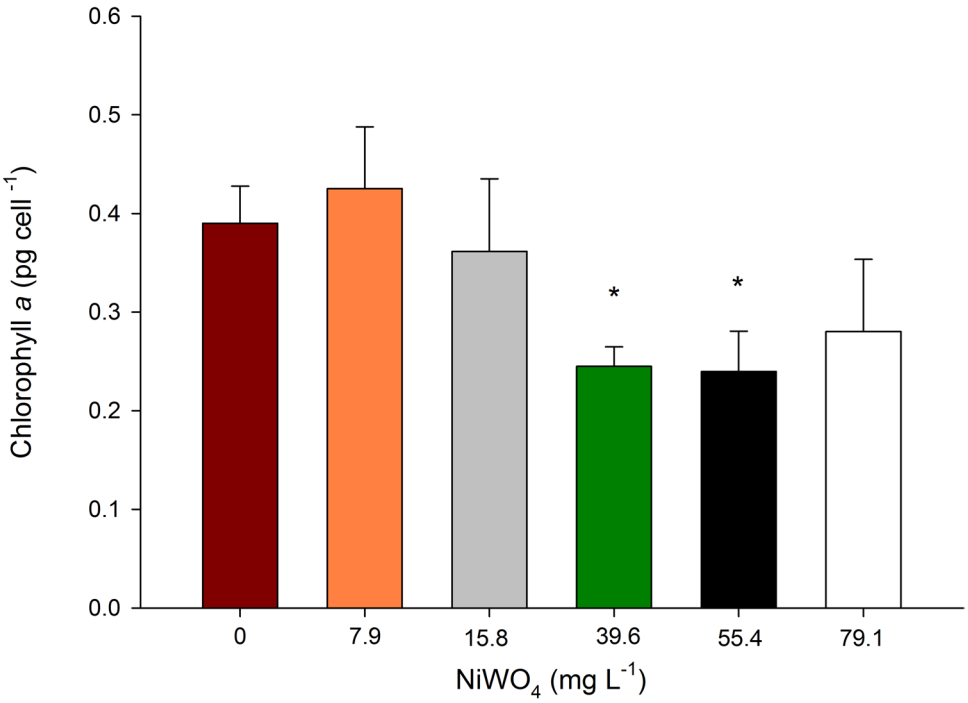

Fig. 6 Chl *a* content of *R. subcapitata* exposed to $NiWO_4$ (mg L^{-1}) NPs for 96 h. Error bars represent the standard deviation, and asterisks represent a significant difference ($p < 0.05$) of treatments compared to the control group

at concentrations of 39.6 and 55.4 mg L^{-1}. According to Martínez-Ruiz and Martínez-Jerónimo (2015), Ni can compromise PS II by interacting with the active site of the oxygen evolving complex, thereby inhibiting electron transport activity (Boisvert et al. 2007). As a result, photosynthetic performance would be compromised, leading to a reduction in chlorophyll content. Since $NiWO_4$ NPs contain Ni and releases Ni^{2+} into the medium, this may explain the observed reduction in Chl *a* content, as corroborated by the decreased $rETR_{max}$ and reduced electron transport (Fig. 5a) particularly at these concentrations, even though there were no significant changes in the OEC. Our data on Chl *a* content are also supported by the reduction in Chl *a* fluorescence (FL3-H), measured by flow cytometry. The relationship between the decrease in Chl *a* content and the reduction in Chl *a* fluorescence (FL3-H) likely reflects the impact of the composite on pigment synthesis (Zhang et al., 2012; Sendra et al. 2017), possibly due to inhibition in the electron transport chain in the donor center (Sendra et al. 2017), which would result in decreased fluorescence.

Therefore, we emphasize the importance of ecotoxicological research that uses multiple endpoints to evaluate the effects of nanoparticles. However, to gain a deeper understanding of the underlying mechanisms of toxicity and the associated risks of these nanoparticles for autotrophic organisms, it would be valuable to assess their toxicity in other strains and species of microalgae, as well as to incorporate long-term studies. Future research should explore the responses of additional microalgal species to $NiWO_4$ nanoparticles.

Conclusion

$NiWO_4$-NPs affected photosynthetic activity and morphological aspects by decreasing chlorophyll *a* fluorescence and altering in cell complexity and size. Initially, we hypothesized that the NPs would cause toxicity to the algal cells with increasing NP concentrations, and that the formation of intracellular ROS would be directly related to toxicity. Surprisingly, the $NiWO_4$ NPs did not impair algal cell growth, nor did they induce negative effects typically associated with ROS. However, we did observe photosynthetic alterations, demonstrated by the reduction in effective yield at 39.6 mg L^{-1}, changes in quenching parameters at concentrations of 39.6 and 79.1 mg L^{-1}, and alterations in light curve parameters. These results highlight that algal cells do not tolerate high light intensities when exposed to NPs. The evaluation of different endpoints provides a comprehensive and important understanding of how *R. subcapitata* cells respond to $NiWO_4$ NPs exposure. Our findings underscore the need for nanotoxicity assessments using a multiple-endpoint approach, as the parameters evaluated in our study reflect different sensitivities. We also emphasize that the effects of NiWO4 NPs on other species of microalga species and on organisms at other trophic levels remain unknown. Therefore, it is essential to evaluate the effects of these NPs on other trophic levels in future research.

Supplementary Information The online version contains supplementary material available at https://doi.org/10.1007/s10123-024-00628-1.

Acknowledgements We would also like to thank Dr. Ana Teresa Lombardi, Dr. Hugo Miguel Preto de Morais Sarmento and Dr. Ana Rita Araújo Nogueira for the permission to use their laboratories, as well as the equipment.

Author Contribution CBA: conceptualization, data curation, methodology, investigation, formal analysis, writing—original draft, writing—review and editing, project administration. RCG: formal analysis, investigation, methodology, writing—review and editing. GSR: formal analysis, methodology, writing—review and editing. ASM: formal analysis, methodology, writing—review and editing. MA: data curation, formal analysis, investigation,, methodology, writing—review and editing. TMP: formal analysis, investigation, writing—review and editing. LSV: formal analysis, investigation, writing—review and editing. AJM: formal analysis, investigation, writing—review and editing. MAS: formal analysis, investigation, writing—review and editing. MGGM: conceptualization, methodology, resources, writing—review and editing. EL: conceptualization, formal analysis, funding acquisition, methodology, resources, supervision, writing, review and editing.

Funding This study was financed, in part, by the São Paulo Research Foundation (FAPESP), Brasil (process number 2013/07296–2, 2018/07988–5), Financiadora de Estudos e Projetos—FINEP, Conselho Nacional de Desenvolvimento Científico e Tecnológico – CNPq, and Coordenação de Aperfeiçoamento de Pessoal de Nível Superior—Brasil (CAPES) – Finance Code 001. CBA and RCG have post-doctoral grants from the São Paulo Research Foundation FAPESP (grant 2021/13607–7 and 2021/13583–0). GSR was supported by Ministry of Research and Universities of the Government of Catalonia and Beatriu de Pinós Programme (Project 2021-BP-00102). ASM was supported by Coordenação de Aperfeiçoamento de Pessoal de Nível Superior – Brasil (CAPES) (finance Code 001 and 88887.364036/2019–00). MA acknowledges the Ministerio de Ciencia e Innovación (Spain) for the Juan de la Cierva fellowship with code JDC2022-049934-I. AJM was supported by São Paulo Research Foundation FAPESP (grant 2022/06219–3) MGGM thanks the CNPq for the research productivity grant (process 316064/2021–1).

Data availability The datasets generated during and/or analyzed during the current study are available from the corresponding author on reasonable request.

Declarations No conflicts, informed consent, human, or animal rights are applicable for this work.

Conflict of interest The authors declare no competing interests.

References

Abreu CB, Gebara RC, dos Reis LL, Rocha GS, Alho LOG, Alvarenga LM, Virtuoso LS, Assis M, da Mansano A, S., Longo, E., & Melão, M. da G. G. (2022) Toxicity of α -Ag 2 WO 4

microcrystals to freshwater microalga *Raphidocelis subcapitata* at cellular and population levels. Chemosphere 288(2021):9–16. https://doi.org/10.1016/j.chemosphere.2021.132536

Abreu CB, Gebara RC, dos Reis LL, Rocha GS, Alho LOG, Alvarenga LM, Virtuoso LS, Assis M, da Mansano A, S., Longo, E., & Melão, M. da G. G. (2022b) Effects of α-Ag2WO4 crystals on photosynthetic efficiency and biomolecule composition of the algae *Raphidocelis subcapitata*. Water Air Soil Pollut 233(4):121. https://doi.org/10.1007/s11270-022-05604-x

AFNOR (1980) Norme experimentale. Essais deseaux Determination de I'nhibition de *Scenedesmus subspicatus* par une substance T90–T304. Paris

Alho LDOG, Gebara RC, de Araujo Paina K, Sarmento H, Melão MDGG (2019) Responses of *Raphidocelis subcapitata* exposed to Cd and Pb: mechanisms of toxicity assessed by multiple endpoints. Ecotoxicol Environ Saf 169:950–959

Alho LDOG, Souza JP, Rocha GS, da Silva Mansano A, Lombardi AT, Sarmento H, Melão MGG (2020) Photosynthetic, morphological and biochemical biomarkers as tools to investigate copper oxide nanoparticle toxicity to a freshwater chlorophyceae. Environ Pollut 265:114856. https://doi.org/10.1016/j.envpol.2020.114856

Almeida C, Gomes T, Habuda-Stanic M, Lomba JAB, Romi´c ˇZ, Turkalj JV, Lillicrap A (2019) Characterization of multiple biomarker responses using flow cytometry to improve environmental hazard assessment with the green microalgae *Raphidocelis subcapitata*. Sci Total Environ J 687:827–838.https://doi.org/10.1016/j.scitotenv.2019.06.124

Alshehri SM, Ahmed J, Alzahrani AM, Ahamad T (2017) Synthesis, characterization, and enhanced photocatalytic properties of NiWO4 nanobricks. New J Chem 41(16):8178–8186. https://doi.org/10.1039/c7nj02085f

Assis MD, Gouveia AF, Ribeiro LK, Ponce MA, Churio MS, Oliveira Jr ON, ... and Andres J (2023) Towards an efficient selective oxidation of sulfides to sulfones by NiWO4 and α-Ag2WO4. Appl Catal: Gen 652, 119038 https://doi.org/10.1016/j.apcata.2023.119038

Azadbakht A, Abbasi AR, Noori N, Rafiee E, Taran M (2013) Synthesis and characterization of nanocrystalline CoWO4@silk fibers with antibacterial activity under ultrasound irradiation. Fibers Polym 14(4):687–692. https://doi.org/10.1007/s12221-013-0687-1

Azqueta A, Dusinska M (2015) The use of the comet assay for the evaluation of the genotoxicity of nanomaterials. Front Genet 6:39. https://doi.org/10.3389/fgene.2015.00239

Baker, N. R. (2008). Chlorophyll fluorescence : a probe of photosynthesis in vivo https://doi.org/10.1146/annurev.arplant.59.032607.092759

Barreto DM, Tonietto AE, Lombardi AT (2021) Environmental concentrations of copper nanoparticles affect vital functions in *Ankistrodesmus densus*. Aquatic Toxicology 231(2020):105720. https://doi.org/10.1016/j.aquatox.2020.105720

Beer C, Foldbjerg R, Hayashi Y, Sutherland DS, Autrup H (2012) Toxicity of silver nanoparticles-nanoparticle or silver ion? Toxicol Lett 208(3):286–292. https://doi.org/10.1016/j.toxlet.2011.11.002

Bian S, Mudunkotuwa IA, Rupasinghe T, and Grassian VH (2011) Aggregation and dissolution of 4 nm ZnO nanoparticles in aqueous environments : influence of pH , ionic strength , size , and adsorption of humic acid. 6059–6068

Boisvert S, Joly D, Leclerc S, Govindachary S, Harnois J, Carpentier R (2007) Inhibition of the oxygen-evolving complex of photosystem II and depletion of extrinsic polypeptides by nickel. Biometals 20(6):879–889. https://doi.org/10.1007/s10534-007-9081-z

Bryan AK, Engler A, Gulati A, and Manalis SR (2012) Continuous and long-term volume measurements with a commercial coulter counter. M(1), 1–8. https://doi.org/10.1371/journal.pone.0029866

Bundschuh M, Seitz F, Rosenfeldt RR, and Schulz R (2016) Effects of nanoparticles in fresh waters : risks , mechanisms and interactions. 2185–2196. https://doi.org/10.1111/fwb.12701

Cosgrove J, Borowitzka MA (2010) Chlorophyll fluorescence terminology: an introduction. In: Suggett DJ, Prášil O, Borowitzka M (eds) Chlorophyll A Fluorescence in Aquatic Sciences: Methods and Applications. Springer, Netherlands, pp 1–17

Danaei M, Dehghankhold M, Ataei S, Davarani FH, Javanmard R, Dokhani A, Khorasani S, and Id MRM (2018) Impact of particle size and polydispersity index on the clinical applications of lipidic nanocarrier systems. 1–17. https://doi.org/10.3390/pharmaceutics10020057

Dewez D, Oukarroum A (2012) Silver nanoparticles toxicity effect on photosystem II photochemistry of the green alga *Chlamydomonas reinhardtii* treated in light and dark conditions. Toxicol Environ Chem 94(8):1536–1546. https://doi.org/10.1080/02772248.2012.712124

Dobias J, Bernier-Latmani R (2013) Silver release from silver nanoparticles in natural waters. Environ Sci Technol 47(9):4140–4146

Filová A, Fargašová A, Molnárová M (2021) Cu, Ni, and Zn effects on basic physiological and stress parameters of Raphidocelis subcapitata algae. Environ Sci Pollut Res 28(41):58426–58441. https://doi.org/10.1007/s11356-021-14778-6

Gebara RC, de Alho L, O. G., Rocha, G. S., da Silva Mansano, A., & Melão, M. da G. G. (2020) Zinc and aluminum mixtures have synergic effects to the algae *Raphidocelis subcapitata* at environmental concentrations. Chemosphere 242:125231

Gebara RC, Alho LDOG, da Silva Mansano A, Rocha GS, Melão MDGG (2023) Single and combined effects of Zn and Al on photosystem II of the green microalgae *Raphidocelis subcapitata* assessed by pulse-amplitude modulated (PAM) fluorometry. Aquat Toxicol 254:106369

Genty B, Briantais J-M, and Baker NR (1989) The relationship between the quantum yield of photosynthetic electron transport and quenching of chlorophyll fluorescence. Biochimica et Biophysica Acta (BBA)-General Subjects, 990(1), 87–92

Gong N, Shao K, Feng W, Lin Z, Liang C, Sun Y (2011) Biotoxicity of nickel oxide nanoparticles and bio-remediation by microalgae Chlorella vulgaris. Chemosphere 83(4):510–516. https://doi.org/10.1016/j.chemosphere.2010.12.059

Gong N, Shao KS, Li GY, Sun YQ (2014) Nickel oxide nanoparticles induce oxi- dative stress and morphological changes on marine *Chlorella vulgaris*. Adv Mater Res 955–959:956–960

Griffitt RJ, Luo J, Gao J, Bonzongo JC, Barber DS (2008) Effects of particle composition and species on toxicity of metallic nanomaterials in aquatic organisms. Environ Toxicol Chem 27(9):1972–1978. https://doi.org/10.1897/08-002.1

Guo R, Lu D, Liu C, Hu J, Wang P, Dai X (2022) Toxic effect of nickel on microalgae Phaeodactylum tricornutum (Bacillariophyceae). Ecotoxicology 31(5):746–760. https://doi.org/10.1007/s10646-022-02532-8

Han ZX, Zhang M (2012) Biotoxicity effects of NiO-Nanoparticles on *Chlorella sp*. In: 2012 International conference on computer distributed control and intelligent environmental monitoring. IEEE, pp 174–177. https://doi.org/10.1109/CDCIEM.2012.48

Herlory O, Bonzom J, Gilbin R (2013) Sensitivity evaluation of the green alga Chlamydomonas reinhardtii to uranium by pulse amplitude modulated (PAM) fluorometry. Aquat Toxicol 140–141:288–294. https://doi.org/10.1016/j.aquatox.2013.06.007

Hong Y, Hu H, Xie X, Sakoda A, Sagehashi M, and Li F (2009) Gramine-induced growth inhibition , oxidative damage and antioxidant responses in freshwater cyanobacterium Microcystis aeruginosa. 91 262–269. https://doi.org/10.1016/j.aquatox.2008.11.014

Ibiapina BR, Lima AE, Ribeiro LK, Cruz-Filho JF, Sales AG, Ramos M A, ... Luz Jr GE (2022) Pyrazinamide photodegradation on NiWO4-palygorskite nanocomposites under polychromatic irradiation. Environ Sci Pollut Res 29(52):79343–79356. https://doi.org/10.1007/s11356-022-21338-z

Jassby AD, Platt T (1976) Mathematical formulation of the relationship between photosynthesis 483 and light for phytoplankton. Limnol Oceanogr 21:540–547

Jeffrey SW, Humphrey GF (1975) New spectrophotometric equations for determining chlorophylls a, b, c1 and c2 in higher plants, algae and natural phytoplankton. Biochem Physiol Pflanz 167(2):191–194. https://doi.org/10.1016/s0015-3796(17)30778-3

Karthiga R, Kavitha B, Rajarajan M, Suganthi A (2015) Photocatalytic and antimicrobial activity of NiWO4 nanoparticles stabilized by the plant extract. Mater Sci Semicond Process 40:123–129. https://doi.org/10.1016/j.mssp.2015.05.037

Ke J, Younis MA, Kong Y, Zhou H, Liu J, Lei L, Hou Y (2018) Nanostructured ternary metal tungstate-based photocatalysts for environmental purification and solar water splitting : a review. Nano-Micro Letters 10(4):1–27. https://doi.org/10.1007/s40820-018-0222-4

Klughammer C, Schreiber U (2008) Complementary PS II quantum yields calculated from simple fluorescence parameters measured by PAM fluorometry and the Saturation Pulse method. PAM Appl Notes 1(1):27–35 (http://www.walz.com/)

Kriedemann PE, Graham RD, Wiskich JT (1985) Photosynthetic dysfunction and in vivo changes in chlorophyll a fluorescence from manganese-deficient wheat leaves. Aust J Agric Res 36(2):157–169. https://doi.org/10.1071/AR9850157

Lekamge S, Miranda AF, Trestrail C, Pham B, Ball AS, Shukla R, Nugegoda D (2019) The toxicity of nonaged and aged coated silver nanoparticles to freshwater alga *Raphidocelis subcapitata*. Environ Toxicol Chem 38(11):2371–2382. https://doi.org/10.1002/etc.4549

Lekamge S, Miranda AF, Abraham A, Ball AS, Shukla R, and Nugegoda D (2020) The toxicity of coated silver nanoparticles to the alga Raphidocelis subcapitata. SN Appl Scihttps://doi.org/10.1007/s42452-020-2430-z

Lemarchand C, Couvreur P, Vauthier C, Costantini D, and Gref R (2003) Study of emulsion stabilization by graft copolymers using the optical analyzer Turbiscan. 254, 77–82https://doi.org/10.1016/S0378-5173(02)00687-7

Levard C, Hotze EM, Lowry GV, Brown GE (2012) Environmental transformations of silver nanoparticles: impact on stability and toxicity. Environ Sci Technol 46(13):6900–6914. https://doi.org/10.1021/es2037405

Li F, Qin Q, Zhang N, Chen C, Sun L, Liu X, Chen Y, Li C, Ruan S (2017) Improved gas sensing performance with Pd-doped WO3·H2O nanomaterials for the detection of xylene. Sens Actuators, B Chem 244:837–848. https://doi.org/10.1016/j.snb.2017.01.063

López XA, Fuentes AF, Zaragoza MM, Díaz Guillén JA, Gutiérrez JS, Ortiz AL, Collins-Martínez V (2016) Synthesis, characterization and photocatalytic evaluation of MWO4 (M = Ni Co, Cu and Mn) tungstates. Int J Hydrogen Energy 41(48):23312–23317. https://doi.org/10.1016/j.ijhydene.2016.10.117

Machado MD, Soares EV (2014) Modification of cell volume and proliferative capacity of *Pseudokirchneriella subcapitata* cells exposed to metal stress. Aquat Toxicol 147:1–6

Machado MD, Soares EV (2024) Features of the microalga *Raphidocelis subcapitata*: physiology and applications. Appl Microbiol Biotechnol 108(1):219

Mani S, Vediyappan V, Chen SM, Madhu R, Pitchaimani V, Chang JY, Liu SB (2016) Hydrothermal synthesis of NiWO4 crystals for high performance non-enzymatic glucose biosensors. Sci Rep 6:2–9. https://doi.org/10.1038/srep24128

Mansano AS, Moreira RA, Dornfeld HC, Freitas EC, Vieira E M, Sarmento H, ... and Seleghim MH (2017) Effects of diuron and carbofuran and their mixtures on the microalgae Raphidocelis subcapitata. Ecotoxicology and environmental safety, 142, 312–321.

Marisa I, Marin MG, Caicci F, Franceschinis E, Martucci A, Matozzo V (2015) In vitro exposure of haemocytes of the clam Ruditapes philippinarum to titanium dioxide (TiO2) nanoparticles: nanoparticle characterisation, effects on phagocytic activity and internalisation of nanoparticles into haemocytes. Mar Environ Res 103:11–17. https://doi.org/10.1016/j.marenvres.2014.11.002

Martínez-ruiz EB, Martínez-jerónimo F (2015) Nickel has biochemical, physiological, and structural effects on the green microalga Ankistrodesmus falcatus : an integrative study. Aquat Toxicol 169:27–36. https://doi.org/10.1016/j.aquatox.2015.10.007

Mattoo AK, Giardi MT, Raskind A, Edelman M (1999) Dynamic metabolism of photosystem II reaction center proteins and pigments. Physiol Plant 107(4):454–461. https://doi.org/10.1034/j.1399-3054.1999.100412.x

Mohamed MM, Ahmed SA, Khairou KS (2014) Unprecedented high photocatalytic activity of nanocrystalline WO3/NiWO4 heterojunction towards dye degradation: effect of template and synthesis conditions. Appl Catal B 150–151:63–73. https://doi.org/10.1016/j.apcatb.2013.12.001

Montini T, Gombac V, Hameed A, Felisari L, Adami G, Fornasiero P (2010) Synthesis, characterization and photocatalytic performance of transition metal tungstates. Chem Phys Lett 498(1–3):113–119. https://doi.org/10.1016/j.cplett.2010.08.026

Nguyen MK, Moon JY, and Lee YC (2020) Microalgal ecotoxicity of nanoparticles: an updated review. Ecotoxicology and Environmental Safety, 201(January). https://doi.org/10.1016/j.ecoenv.2020.110781

Nogueira V, Lopes I, Rocha-Santos TAP, Rasteiro MG, Abrantes N, Gonçalves F, Soares AMVM, Duarte AC, Pereira R (2015) Assessing the ecotoxicity of metal nano-oxides with potential for wastewater treatment. Environ Sci Pollut Res 22(17):13212–13224. https://doi.org/10.1007/s11356-015-4581-9

Oukarroum A, Bras S, Perreault F, Popovic R (2012) Inhibitory effects of silver nanoparticles in two green algae, *Chlorella vulgaris* and *Dunaliella tertiolecta*. Ecotoxicol Environ Saf 78:80–85.https://doi.org/10.1016/j.ecoenv.2011.11.012

Oukarroum A, Barhoumi L, Samadani M, and Dewez D (2015) Toxic effects of nickel oxide bulk and nanoparticles on the aquatic plant lemna gibba L. BioMed Research International, 2015(Ii). https://doi.org/10.1155/2015/501326

Oukarroum A, Zaidi W, Samadani M, and Dewez D (2017) Toxicity of nickel oxide nanoparticles on a freshwater green algal strain of chlorella vulgaris. BioMed Res Int 2017(2011). https://doi.org/10.1155/2017/9528180

Panneerselvam K, Rudragouda S, Mohan M (2018) Toxicity of nickel on the selected species of marine diatoms and copepods. Bull Environ Contam Toxicol 100(3):331–337. https://doi.org/10.1007/s00128-018-2279-7

Peters A, Merrington G, Schlekat C, De Schamphelaere K, Stauber J, Batley G, Harford A, van Dam R, Pease C, Mooney T, Warne M, Hickey C, Glazebrook P, Chapman J, Smith R, Krassoi R (2018) Validation of the nickel biotic ligand model for locally relevant species in Australian freshwaters. Environ Toxicol Chem 37:2566–2574. https://doi.org/10.1002/etc.4213

Pourmortazavi SM, Rahimi-Nasrabadi M, Khalilian-Shalamzari M, Zahedi MM, Hajimirsadeghi SS, Omrani I (2012) Synthesis, structure characterization and catalytic activity of nickel tungstate nanoparticles. Appl Surf Sci 263:745–752. https://doi.org/10.1016/j.apsusc.2012.09.153

Qian H, Zhu K, Lu H, Lavoie M, Chen S, Zhou Z, Deng Z, Chen J, Fu Z (2016) Contrasting silver nanoparticle toxicity and

detoxification strategies in Microcystis aeruginosa and *Chlorella vulgaris*: new insights from proteomic and physiological analyses. Sci Total Environ 572:1213–1221. https://doi.org/10.1016/j.scitotenv.2016.08.039

Reis LL, Alho L de OG, de Abreu CB, and Melão M da GG (2021) Using multiple endpoints to assess the toxicity of cadmium and cobalt for chlorophycean Raphidocelis subcapitata. Ecotoxicol Environ Safety 208 111628

Reis LL, Alho L. de OG, de Abreu CB, Gebara R C, Mansano A. da S, and Melão M da GG (2022) Effects of cadmium and cobalt mixtures on growth and photosynthesis of Raphidocelis subcapitata (Chlorophyceae). Aquatic Toxicol 244(2021) 106077 https://doi.org/10.1016/j.aquatox.2022.106077

Reis LL, de Abreu CB, Gebara RC, Rocha GS, Longo E, Mansano ADS, Melão MDGG (2024) Isolated and combined effects of cobalt and nickel on the microalga *Raphidocelis subcapitata*. Ecotoxicology. https://doi.org/10.1007/s10646-024-02728-0. Epub ahead of print. PMID: 38236330

Rocha GS, Lombardi AT, Espíndola ELG (2021) Combination of P-limitation and cadmium in photosynthetic responses of the freshwater microalga *Ankistrodesmus densus* (Chlorophyceae). Environ Pollut 275:116673. https://doi.org/10.1016/j.envpol.2021.116673

Rosal FJO, Gouveia AF, Sczancoski JC, Lemos PS, Longo E, Zhang B (2018) Electronic structure, growth mechanism, and sonophotocatalytic properties of sphere-like self-assembled NiWO 4 nanocrystals. Inorg Chem Commun 98:34–40. https://doi.org/10.1016/j.inoche.2018.10.001

Sarmento H, Unrein F, Isumbisho M, Stenuite S, Gasol JM, DESCY, J. (2008) Abundance and distribution of picoplankton in tropical, oligotrophic Lake Kivu, eastern Africa. Freshw Biol 53(4):756–771

Schreiber USCHLIWA, Schliwa U, Bilger W (1986) Continuous recording of photochemical and non-photochemical chlorophyll fluorescence quenching with a new type of modulation fluorometer. Photosynth Res 10:51–62. https://doi.org/10.1007/BF00024185

Schreiber UBWN, Bilger W, Neubauer C (1995) Chlorophyll fluorescence as a nonintrusive indicator for rapid assessment of in vivo photosynthesis. In: Ecophysiology of photosynthesis. Berlin, Heidelberg, Springer Berlin Heidelberg, pp 49–70

Sendra M, Yeste MP, Gatica JM, Moreno-Garrido I, Blasco J (2017) Direct and indirect effects of silver nanoparticles on freshwater and marine microalgae (*Chlamydomonas reinhardtii* and *Phaeodactylum tricornutum*). Chemosphere 179:279–289

Shanmugapriya S, Surendran S, Nithya VD, Saravanan P, Kalai Selvan R (2016) Temperature dependent electrical and magnetic properties of CoWO4 nanoparticles synthesized by sonochemical method. Mater Sci Eng b: Solid-State Mater Adv Technol 214:57–67. https://doi.org/10.1016/j.mseb.2016.09.002

Shoaf WT, Lium BW (1976) Improved extraction of chlorophyll a and b from algae using dimethyl sulfoxide. Limnol Oceanogr 21(6):926–928. https://doi.org/10.4319/lo.1976.21.6.0926

Sousa CA, Soares HMVM, Soares EV (2018) Toxic effects of nickel oxide (NiO) nanoparticles on the freshwater alga *Pseudokirchneriella subcapitata*. Aquat Toxicol 204(July):80–90. https://doi.org/10.1016/j.aquatox.2018.08.022

Stensberg MC, Wei Q, Mclamore ES, Marshall D (2011) Toxicological studies on silver nanoparticles: challenges and oopportunities in assessment, monitoring and imaging. Nanomedicine 6(5):879–898. https://doi.org/10.2217/nnm.11.78

Suzuki H, Toyooka T, Ibuki Y (2007) Simple and easy method to evaluate uptake potential of nanoparticles in mammalian cells using a flow cytometric light scatter analysis. Environ Sci Technol 41:3018–3024

Ungelenk J, Speldrich M, Dronskowski R and Feldmann C (2014) Polyol-mediated low-temperature synthesis of crystalline tungstate. 31, 62–69https://doi.org/10.1016/j.solidstatesciences.2014.02.020

Zhang W, Zhang M, Lin K, Sun W, Xiong B, Guo M, ... Fu R (2012) Eco-toxicological effect of Carbamazepine on *Scenedesmus obliquus* and *Chlorella pyrenoidosa*. Enviro Toxicol Pharmacol 33(2):344–352. https://doi.org/10.1016/j.etap.2011.12.024

Zhang CL, Jiang HS, Gu SP, Zhou XH, Lu ZW, Kang XH, Yin L, Huang J (2019) Combination analysis of the physiology and transcriptome provides insights into the mechanism of silver nanoparticles phytotoxicity. Environ Pollut 252:1539–1549. https://doi.org/10.1016/j.envpol.2019.06.032